

# Lightning protection for power transformers of Aqaba Thermal Power Station

Wael Fawzi Abu Shehab<sup>1</sup> , Shehab Abdulwaddood Ali<sup>2</sup>,  
Mohammad Ibrahim Alsharari<sup>1</sup>

<sup>1</sup>*Department of Electrical Engineering, Al-Hussein Bin Talal University  
P.O. Box 20, Postal Code 71111, Ma'an, Jordan  
e-mail: {waelabushehab/sharari.m.i}@ahu.edu.jo*

<sup>2</sup>*College of Saber, University of Aden, Yemen  
e-mail: shehababdulwaddood@gmail.com*

(Received: 30.01.2020, revised: 08.04.2020)

**Abstract:** In this paper, a study of the lightning phenomenon and its harmful effect on Aqaba Thermal Power Station (ATPS), located in the south-western border of Jordan, is presented using the Electromagnetic Transients Program – Alternative Transients Program (EMTP-ATP). This study has been arisen due to an installation need of appropriate lightning arresters (LAs) for the 15/410 kV step-up transformers of the ATPS to eliminate the destructive effect of lightning. The simulation is carried out for two cases, once without using LAs and once more with using them. Two scenarios are applied for each of these cases, once when lightning strikes the primary side of the transformer and once more when it strikes the secondary side. The results obtained by the simulation indicate the necessity of LAs installation. This study, with using the EMTP-ATP program, is done for the first time with additional details that help researchers, designers, and engineers to get a broad overview of the ATPS in order to protect it against lightning.

**Key words:** basic insulation level BIL, EMTP-ATP program, lightning, lightning arrester LA, metal oxide varistor MOV

## 1. Introduction

An electrical surge or a spike is a temporary very short rise in voltage or current that can appear on power systems. A lightning strike is one of the reasons that cause high-magnitude electrical surges and is one of the primary causes of blackouts, related to probabilistic failures [1].



© 2020. The Author(s). This is an open-access article distributed under the terms of the Creative Commons Attribution-NonCommercial-NoDerivatives License (CC BY-NC-ND 4.0, <https://creativecommons.org/licenses/by-nc-nd/4.0/>), which permits use, distribution, and reproduction in any medium, provided that the Article is properly cited, the use is non-commercial, and no modifications or adaptations are made.

A single bolt of lightning can generate about 200 MV [1]. A destructive surge can be initiated and propagated over power lines not only due to lightning that strikes a power line or its supporting towers, but also nearby lightning strikes can induce a surge of 30 kA or more in power lines [2].

About 80% of lightning flashes contain multiple strokes. Three to five strokes are common. Typically, the individual strokes are separated by 40 to 50 ms. Strokes subsequent to the first are called subsequent strokes. Peak currents of the subsequent stroke are typically 10 to 15 kA, while currents of the first stroke are typically near 30 kA. The current rise times (measured between 10% and 90% of the peak value) of subsequent strokes are generally less than one microsecond, whereas rise times of the first stroke are some microseconds. Fig. 1 shows curves representing a typical first and a typical subsequent stroke transferring negative charge from cloud to ground [3]. Data of the most important parameters of lightning strokes collected by some researchers can be found in [4–6].

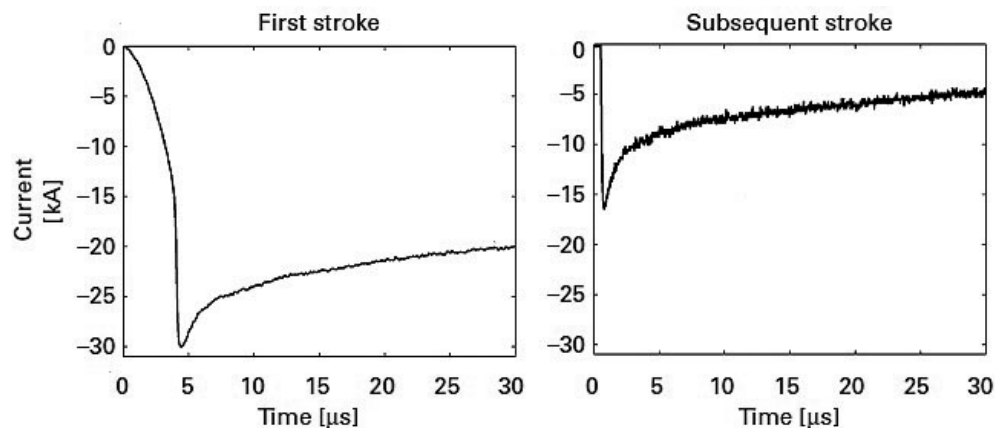


Fig. 1. Typical first and subsequent stroke

To intercept and disperse the lightning current harmlessly to earth, lightning protection of a power line should be used. It can be achieved by using a protective grounded conductor above the power line so that the lightning current is shunting to ground. Lightning rods and overhead ground wires on power lines are the most common examples of the protective conductors. In addition to the structural protection of power lines discussed above, electrical and electronic equipment connected to the power lines should be protected from the voltages resulting from lightning-induced signals. This protection can be achieved by filtering out these voltages, using isolating devices, or using surge protective devices (SPDs) called lightning arresters (LAs) [3].

One of the most common LAs is the metal oxide varistor (MOV). It is a voltage-dependent resistor that is made from metal oxide particles. When the voltage level in the power line is at the rated voltage, the MOV has a very high resistance and it conducts very little current. If the voltage level approaches breakdown, the MOV's resistance decreases and begins to conduct current. At voltages above the breakdown, the extra current is diverted to ground.

Several researches dealt with analysis and simulation of lightning and its effect on power lines. Researchers in [7] evaluated several methods (by using overhead ground wire and surge arrester) of decreasing the outage rate caused by lightning strikes directly to distribution lines. Analysis for the lightning overvoltage performance of substations are performed in [8–9], considering various critical parameters, such as the installation position of the arresters, the grounding resistance, and the length of the underground cable that connects the transmission line with the transformer. In [10], study of the lightning overvoltage protection of large power transformers is presented, where the main focus has been put on the earth grid. A review of the most important models for metal oxide surge arresters can be found in [11], where the models are used to estimate the lightning performance of transmission lines.

In this paper, the effect of lightning on 15/410 kV transformers, which are located in Aqaba Thermal Power Station (ATPS), is modeled and simulated using the Electromagnetic Transients Program- Alternative Transients Program (EMTP-ATP) ver. 6.2. The study has been arisen due to the installation need of appropriate LAs for the step-up transformers of the ATPS to eliminate the destructive effect of lightning. The simulation is carried out for two cases, once without using LAs and once more with using them. This study, with using the EMTP-ATP program, is done for the first time with additional details that help researchers, designers, and engineers to get a broad overview of the ATPS in order to protect it against lightning.

The paper is structured as follows. Sections 2 and 3 present lightning flash and lightning arrester models, respectively. Section 4 is devoted to the technical data of the ATPS and its modeling using the EMTP-ATP program. Section 5 discusses simulation results. Finally, section 6 concludes the paper.

## 2. Lightning flash model

A 10/350  $\mu$ s one-stroke lightning flash with amplitude 30 kA is simulated in the EMTP-ATP program using a Heidler type-15 [12], which is defined by the function:

$$i(t) = Amp \cdot \frac{(t/T_f)^n}{1 + (t/T_f)^n} \cdot e^{-t/\tau}, \quad (1)$$

where  $Amp$  is the peak value of the lightning stroke,  $T_f$  is the front duration,  $\tau$  is the stroke duration, where the amplitude fell to 37% (tail time), and  $n$  is the factor influencing the rate of the rise of the function (steepness). The lightning stroke is shown in Fig. 2 and its parameters are tabulated in Table 1.

Table 1. Values of Heidler type-15 surge function

Amplitude [kA]	$T_f$ [ $\mu$ s]	$\tau$ [ $\mu$ s]	n	T-start [ms]	T-stop [ms]
30	10	350	2	20	20.35

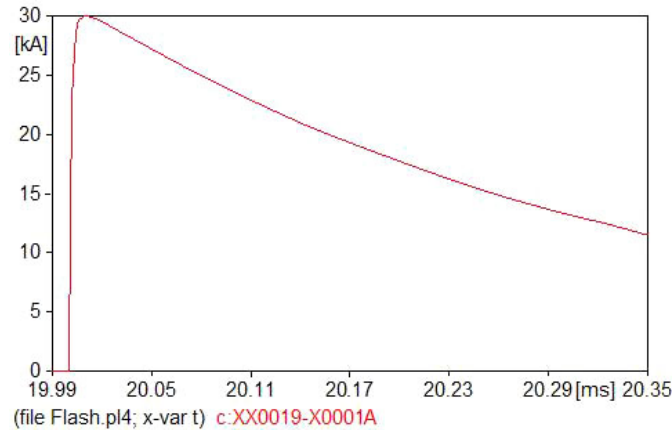


Fig. 2. The lightning stroke (30 kA)

### 3. Lightning arrester model

In this paper, a conventional model which is offered by the EMTP-ATP program is used. It can be simulated by the MOV Type-92 component [12]. It is a non-linear exponential resistor for which the voltage-current (V-I) characteristic can be represented by an arbitrary number of exponential segments, each of them defined by Equation (2) [13].

$$i = p \left( \frac{v}{V_{\text{ref}}} \right)^q, \quad (2)$$

where  $i$  and  $v$  are the arrester current and voltage, respectively.  $p$  and  $q$  are the constants of the device.  $V_{\text{ref}}$  is the arbitrary reference voltage that normalizes the equation and prevents numerical overflow during exponentiation.

The LAs supposed to be used in this paper are similar to two types of Siemens LAs described as follows:

- Type 3EP5, with porcelain housing, class 3, maximum system voltage  $U_s$  (24 kV), rated voltage  $U_r$  (21 kV), continuous operating voltage  $U_c$  (16.8 kV). This type is used for the primary side (15 kV) of the transformer as discussed in section 4.
- Type 3EP6, with porcelain housing, class 5, maximum system voltage  $U_s$  (800 kV), rated voltage  $U_r$  (580 kV), continuous operating voltage  $U_c$  (464 kV). This type is used for the secondary side (410 kV) of the transformer as discussed in section 4.

The two types have been successfully tested to the latest ANSI/ IEEE Standard C62.11-1999. The characteristics of the arresters are listed in Table 2 for the closest values of both voltage levels (15 kV and 410 kV). Fig. 3 shows the residual voltage curves of the arresters, where the residual voltage is chosen for 8/20  $\mu$ s. Table 3 shows further additional data [14].

The maximum continuous operating voltage (MCOV or  $U_c$ ) is an alternating current (AC) rating and should in all circumstances be higher than the maximum line-to-ground voltage of the system to which it will be applied. In some circumstances, due to higher temporary overvoltage

Table 2. Electrical characteristics of 3EP5 and 3EP6 arresters

Type	$U_c$ [kV]	$U_r$ [kV]	Residual voltage at specified discharge current [kV]						
			30/60 $\mu$ s 0.5 kA	30/60 $\mu$ s 1 kA	30/60 $\mu$ s 2 kA	8/20 $\mu$ s 5 kA	8/20 $\mu$ s 10 kA	8/20 $\mu$ s 20 kA	8/20 $\mu$ s 40 kA
3EP5	16.8	21	40.3	41.3	43.3	47.4	50.4	55.9	63.5
3EP6	464	580	1 083	1 116	1 148	1 233	1 305	1 422	1 553

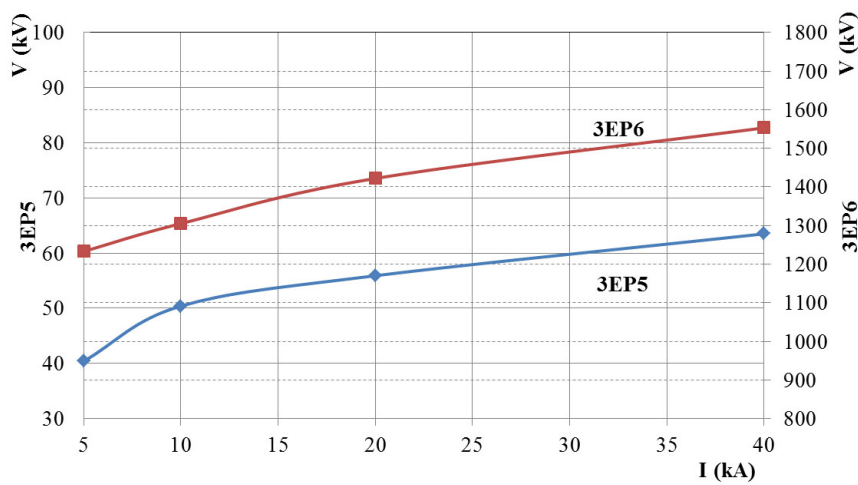


Fig. 3. Residual voltage curves of 3EP5 and 3EP6 arresters

Table 3. Additional data of 3EP5 and 3EP6 arresters

Characteristic	3EP5	3EP6
Long duration current impulse [A]	1 100	2 000
High current impulse [kA]	100	100
Nominal discharge current [kA]	10	20
Rated short-circuit current [kA]	40	65
Energy absorption capability [kJ/kV <sub>r</sub> ]	8	14

(TOV) conditions, the MCOV may need to be increased on the arrester, but it should never be decreased below the steady-state line-to-ground voltage of the system.

The arrester must be connected as close as possible to the equipment, but due to the layout requirements, the arrester may not be installed near the power transformer. The distance between the transformer and the point where the arrester is connected  $L_1$  may vary from 0 to 40 m [15]. In this study,  $L_1$  is chosen to be 15 m. The length of the conductor that connects the line with

the arrester  $L_2$  may vary from 1 to 3 m.  $L_2$  is chosen to be 3 m in the study. Finally, a grounding conductor of length  $L_3 = 5$  m is connected between the arrester and the ground via a  $1 \Omega$  resistor. All these connections are modeled by an inductance of  $1 \mu\text{H/m}$ .

#### 4. ATPS modeling using the EMTP-ATP program

This paper presents a study of ATPS transformer protection from lightning. The ATPS is a 650 MW power station located on the south-western border of Jordan. It consists of five steam turbines units ( $5 \times 130$  MW). The studied case corresponds to a part of the ATPS (units No. 3, 4 and 5) as shown in Fig. 4. Each of these units has a 3-phase 50 Hz generator rated at 160 MVA, 15 kV. The generators (labeled G3, G4, and G5) supply a 400 kV network (labeled BB1 and BB2) through 15/410 kV step-up transformers (labeled GTR 3, GTR 4, and GTR 5). The transformers are located outside in open air and connected to the network by 30 m long underground cables. The 400 kV transmission line represents the connection between the ATPS and Amman South Substation (ASS) in Al Muqabalayn town, which is about 320 km long. 15/6.6 kV step-down transformers (labeled UAT 3, UAT 4, and UAT 5) are used only for internal purposes related to the operation of the units themselves. It is good to mention here that units No. 1 and 2, which are not used in this study, supply a 132 kV network.

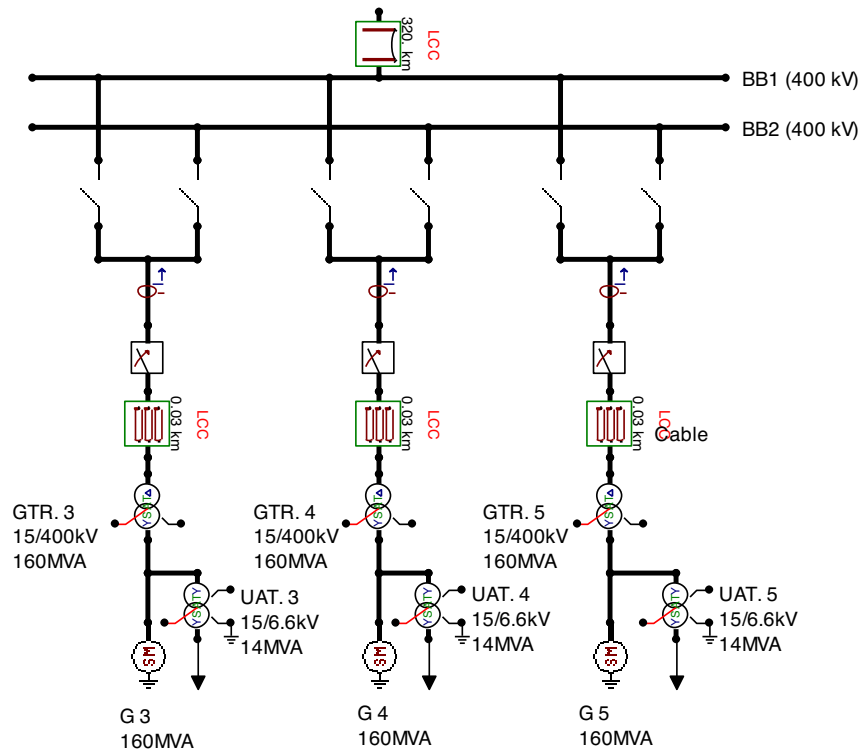


Fig. 4. The three units in the ATPS, which supply a 410 kV network

The effect of lightning on the power system shown in Fig. 4 will be applied only on unit No. 3 at the transformer GTR 3. Two cases will be analyzed, the first one before using LAs and the second one after their use. Each of these cases will have two scenarios concerning lightning contact locations, described as follows:

- Scenario (1): Lightning strikes directly phase A at the primary side of the transformer GTR3.
- Scenario (2): Lightning strikes directly phase A at the secondary side of the transformer GTR3.

The models discussed in the previous sections (2 and 3) are applied to these scenarios.

#### 4.1. Technical data required for modelling

In this section, technical data of the generator and the transformer contained in unit No. 3 are collected and presented (units No. 4 and 5 have identical data as No. 3). Also, data concerning the 400 kV transmission line, as well as the underground cable between this line and the transformer, are presented.

##### 4.1.1. The generator

The generator in unit No. 3 is a Y-connection synchronous generator type WX21Z-092LLT, manufactured by ABB Power Generation Ltd. Its rated power, voltage, and power factor are 160 MVA, 15 kV, and 0.85, respectively [16]. This generator is represented by the SM59 model in the EMTP-ATP program [12], with input data shown in Table 4. The voltage magnitude is calculated as in Equation (3) [17].

$$V_{amp} = \sqrt{2/3} \times 15 \text{ kV} = 12.247 \text{ [kV]}. \quad (3)$$

SMOVTP and SMOVTQ (Table 4) are proportionality factors used only to split the real power and reactive power, respectively among multiple machines in parallel during initialization. No machine in parallel corresponds to SMOVTP = 1 and SMOVTQ = 1.

##### 4.1.2. The transformers

In the ATPS unit No. 3, the used transformer is a step-up 15/410 kV 30BAT01 manufactured by ABB. It is an outdoor transformer with 3-legged stacked core. The step-down 15/6.6 kV transformer is used only for internal purposes as mentioned earlier. Both transformers are represented by the SATTRAFO model in the EMTP-ATP program with input data shown in Table 5 [18, 19], where  $R_p$  and  $L_p$  are the resistance and inductance in the primary winding, respectively.  $R_s$  and  $L_s$  are the resistance and inductance in the secondary winding, respectively. Stray capacitances representing a high frequency transformer model [20] are added as shown in Fig. 5 (section 4.2).

##### 4.1.3. The underground cable

The underground power cable used to connect the transformer described in the previous section to the 400 kV transmission line has the technical data tabulated in Table 6 [21]. This cable can be modeled in the EMTP-ATP program by the JMarti component [12].

Table 4. Technical data of the generator

Voltage magnitude [kV]	Frequency [Hz]	Voltage phasor angle phase A [deg.]	Number of poles	SMOVTP
12.247	50	0	2	1
SMOVTP	RMVA [MVA] 3-phase volt-ampere rating	RkV [kV] line-to-line voltage	AGLINE [A] Value of field current which produces rated armature voltage on d-axis	RA [pu] Armature resistance
1	160	15	1243	0
XL [pu] Armature leakage reactance	Xd [pu] Direct-axis synchronous reactance	Xq [pu] Quadrature-axis synchronous reactance	Xd' [pu] D-axis transient reactance	Xq' [pu] Q-axis transient reactance
0.13	1.619	1.539	0.195	0.225
Xd'' [pu] D-axis subtransient reactance	Xq'' [pu] Q-axis subtransient reactance	Tdo' [s] D-axis transient time constant	Tqo' [s] Q-axis transient time constant	Tdo'' [s] D-axis subtransient time constant
0.12	0.2	8.166	7.1	0.022
Tqo'' [s] Q-axis subtransient time constant	Xo [pu] Zero-sequence reactance	RN [pu] Real part of neutral grounding impedance	XN [pu] Imaginary part of neutral grounding impedance	XCAN [pu] Canay's characteristic reactance
0.07	0.067	0	0	0.13
HICO [million kg-m <sup>2</sup> ] Moment of inertia of mass	DSR [(N.m)/(rad/sec)] Speed-deviation self-damping coefficient	DSD [(N.m)/(rad/sec)] Absolute-speed self-damping coefficient	FM Time constants based on short circuit measurements	MECHUN 0: English units 1: Metric units
0.0156	0	0	3	1

Table 5. Technical data of transformers

	Power [MVA]	Voltage [kV]	Connection	R <sub>p</sub> [Ω]	R <sub>s</sub> [Ω]	L <sub>p</sub> [mH]	L <sub>s</sub> [mH]
Step-up	160	15/410	Ynd 11	0.003	1.06	0.469	350
Step-down	14	15/6.6	Y-Y	0.168	0.033	5.36	1

Table 6. Technical data of the cable

Manufacturer	Type	Nominal cross section [mm <sup>2</sup> ]	Number of cores	Conductor material
ABB	Low-Pressure Oil Filled (LPOF)	1 000	1	Annealed copper
Conductor outer diameter [mm]	Conductor insulation material	Insulation thickness [mm]	Armour material	Armour thickness [mm]
42.5	Carbon black paper and metalized paper	27.5	Lead alloy	3.8
Overall diameter of completed cable [mm]	Length [m]	Resistance R [Ω/km]	Inductance L [mH/km]	Capacitance C [F/km]
118	30	0.0236	0.39	0.23
Rho: Resistivity of the conductor material [Ωm]	mu: Relative permeability of the conductor material	mu(ins): Relative permeability of the insulator material outside the conductor	eps(ins): Relative permittivity of the insulator material outside the conductor	
1.7E-8	1	1	2.7	

#### 4.1.4. The transmission line

The 400 kV overhead transmission line between the ATPS and ASS is 320 km long. It is a double circuit 3-phase line with  $2 \times 600 \text{ mm}^2$  cross sectional area aluminum alloy conductors per phase. The spacing between the twin-bundled conductors is 50 cm. Also, the line is with two No. 7 AWG aluminum clad steel overhead earth wires [22]. The parameters and the location of the conductors on the tower are given in Table 7. The transmission line is modeled in the EMTP-ATP program by the LCC module as the 3-phase JMarti type [12]. The ground resistivity (Rho) is assumed to be 100 Ωm and the frequency (Freq. init) at which the line parameters are calculated is 0.005 Hz.

Table 7. The parameters and the location of the conductors on the tower

Phase no.	Resistance [Ω/km]	Reactance [Ω/km]	Outer radius [cm]	Horiz [m]	VTower [m]	VMid [m]
1 (2×)	0.0496	0.3	1.608	±8	44.29	32.14
2 (2×)	0.0496	0.3	1.608	±11.3	33.29	21.14
3 (2×)	0.0496	0.3	1.608	±8.8	23.79	10.64
0 (2×)	0.05	0.43	0.353	±6	52.05	42

In Table 7, Horiz is the horizontal distance between the conductor and the tower center, VTower is the vertical conductor height at the tower, and VMid is the vertical conductor height at the mid-span.

Another crucial elements in a study of lightning overvoltage protection could be modeled by means of surge capacitance [23], such as the following elements appearing in Fig. 5: circuit breakers (CB: 50 pF), current transformers (CT: 200–800 pF), power transformers (1–6 nF) and capacitive voltage transformers (CVT: 4.4 nF).

#### 4.2. Modeling the lightning effect on the ATPS

Using all of the models described in sections 2, 3, and 4, the EMTP-ATP program model of the lightning effect on the ATPS can be assembled as shown in Fig. 5.

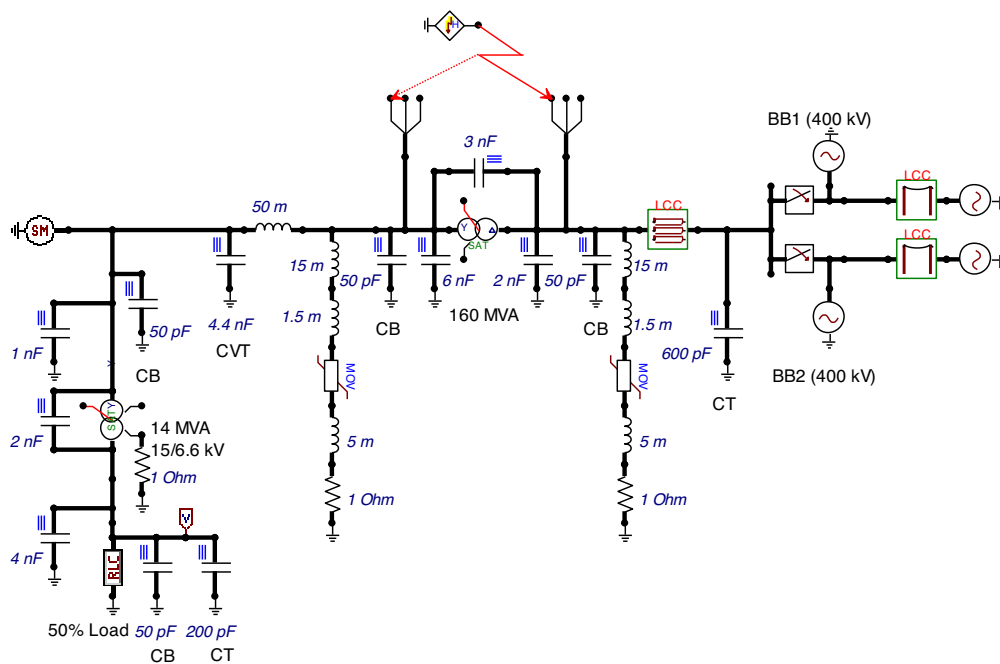


Fig. 5. The EMTP-ATP model of lightning effect on unit No. 3

The effect of lightning is applied only on unit No. 3 at the transformer GTR 3, as mentioned previously. In the next section, the results of this effect will be discussed before and after using LAs according to the scenarios mentioned at the beginning of section 4.

### 5. Results and discussion

Before presenting and discussing the results of the study, the transformer basic insulation level (BIL) should be taken into consideration. It is a certain level to which the transformer is capable to withstand surge voltages without damage. According to [24], the BIL for 15 kV is 95 ~ 110 kV and it is 1425 ~ 1675 kV for 500 kV (900 ~ 1175 for 345 kV). In this study, the BIL is taken from the transformer datasheet as 1425 kV for the high voltage winding and as 125 kV for the low voltage winding.

It is important here to set correctly a time step ( $\Delta T$ ) in simulation settings in the EMT-ATP program to get satisfied and clear results, mainly when the peak voltages due to lightning overreached the BIL of the transformer. In this simulation,  $\Delta T$  was set to  $10^{-6}$  seconds.

The results of the two cases mentioned in section 4 are discussed as follows:

**Case (1):** Without using the LAs.

**Scenario (1):** Lightning hits phase A at the primary side of the transformer.

Fig. 6 and Table 8 show the voltages of the phases at the primary and secondary sides of the transformer when scenario (1) of case (1) is applied. It is very clear that the maximum voltages of the 3 phases (A, B and C) at the primary side reach very high values (A: 4.2 MV, B: 2.1 MV, C: 1.8 MV), which exceed the BIL (125 kV). The secondary side of the transformer is also affected by the lightning flash as shown in Fig. 6, but the maximum voltages of the three phases (A: 1 MV, B: -0.557 MV, and C: -0.527 MV) are still under the BIL (1425 kV). The values in bold in Table 8 indicate overreaching of the transformer BIL.

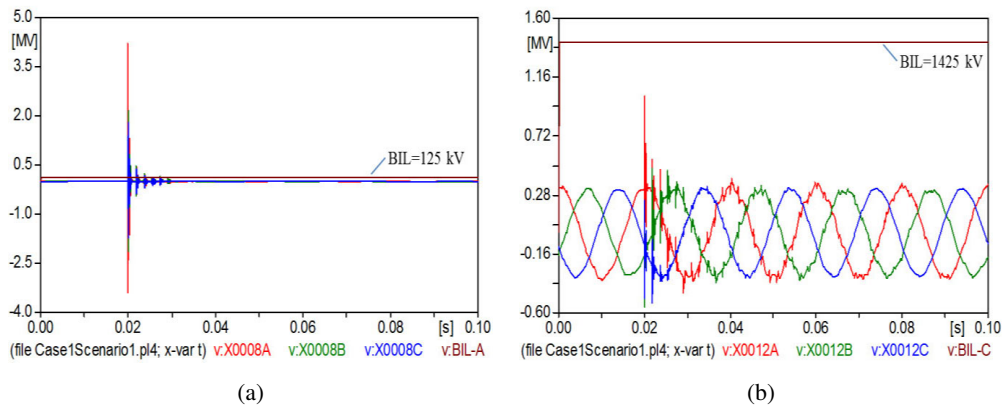


Fig. 6. 3-phase voltages at the primary side (a) and secondary side (b) (scenario (1) of case (1))

Table 8. Maximum voltages due to case (1)

Transformer side	BIL [kV]	Maximum voltage [MV]					
		Scenario (1)			Scenario (2)		
		Phase					
		A	B	C	A	B	C
Primary	125	<b>4.2</b>	<b>2.1</b>	<b>1.8</b>	<b>-0.717</b>	<b>0.430</b>	<b>-0.460</b>
Secondary	1425	1	-0.557	-0.527	<b>-7.68</b>	<b>4.05</b>	<b>-2.58</b>

**Scenario (2):** Lightning hits phase A at the secondary side of the transformer.

Fig. 7 and Table 8 show the 3-phase voltages at the primary and secondary sides of the transformer when scenario (2) of case (1) is applied. It is noted that the maximum values of the voltages at the primary side (A: 717 kV, B: 430 kV, C: 460 kV) are all over the BIL (125 kV).

Similarly, the maximum values of the voltages at the secondary side (A:  $-7.68$  MV, B:  $4.05$  MV, C:  $-2.58$  MV) exceed the BIL ( $1.425$  MV).

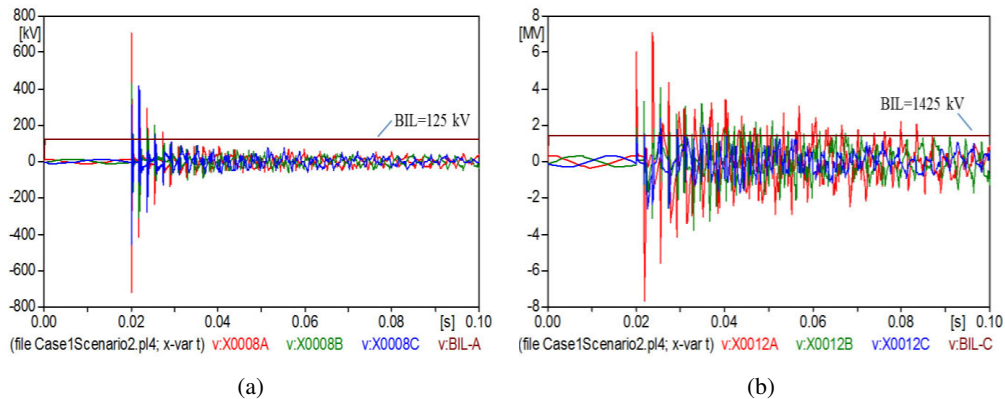


Fig. 7. 3-phase voltages at the primary side (a) and secondary side (b) (scenario (2) of case (1))

### Case (2): With using LAs.

According to the results in case (1), it is necessary to install the LAs, described in section 3, to avoid the destructive effects of lightning. By observing Fig. 8, Fig. 9 and Table 9, it is obvious that the values of maximum voltages are significantly reduced due to the LAs use and are within the BIL rating. When scenario (1) of case (2) is applied, the value of maximum voltage of phase A at the primary side is about  $97.23$  kV as shown in Fig. 8, while maximum voltages of phases B and C are negligible in comparison with the BIL value. This is indicated by sign (-) in Table 9. At the secondary side, all phases have also maximum voltages that are negligible in comparison with the BIL value.

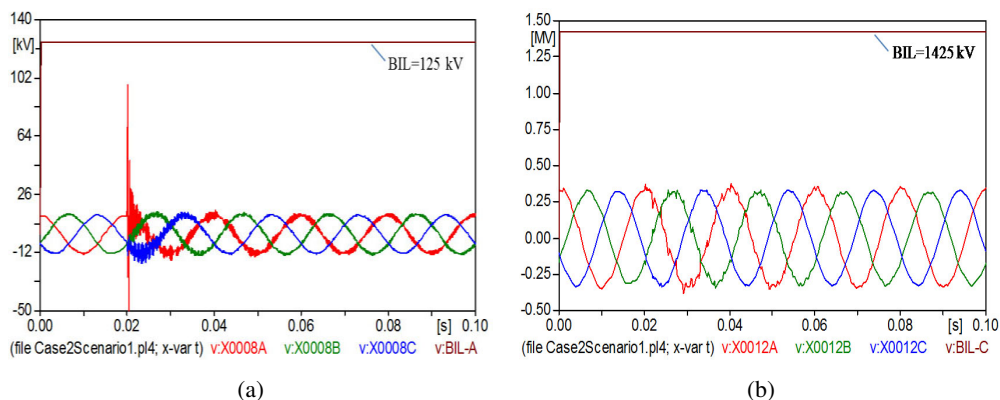


Fig. 8. 3-phase voltages at the primary side (a) and secondary side (b) (scenario (1) of case (2))

For scenario (2) of case (2), the voltages at the primary side have negligible values in comparison with the BIL value as shown in Fig. 9. At the secondary side, the voltage of phase

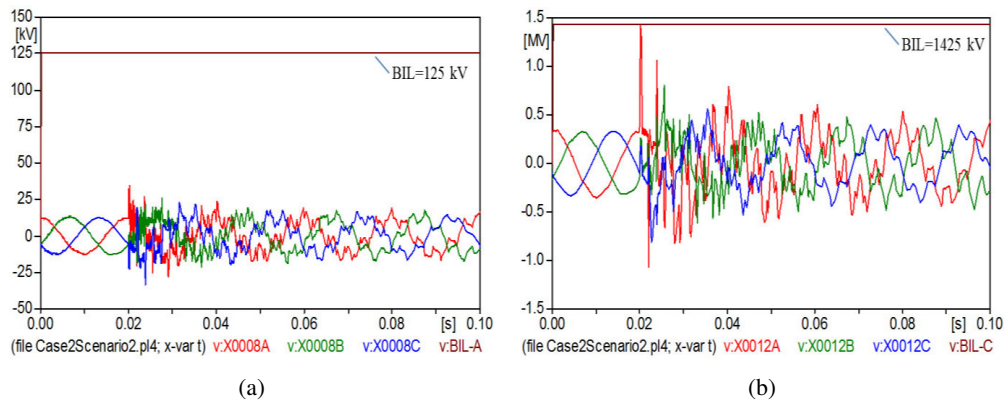


Fig. 9. 3-phase voltages at the primary side (a) and secondary side (b) (scenario (2) of case (2))

Table 9. Maximum voltages due to case (2)

Transformer side	BIL [kV]	Maximum voltage [kV]					
		Scenario (1)			Scenario (2)		
		Phase					
		A	B	C	A	B	C
Primary	125	97.23	–	–	–	–	–
Secondary	1 425	–	–	–	1 424	797	–813

A has a value close to the BIL value (A: 1424 kV), but still within it. This is also applied to the other phases at the secondary side (B: 797 kV, C: –813 kV).

These results indicate the ability of the LAs to immediately reduce lightning effect on the power system. Here, it must be taken into account that the results depend on choosing the suitable LAs and their placement across the system.

Finally, the energy dissipated by the arresters according to both scenarios of case (2) is shown in Table 10. For scenario (1), only the arrester 3EP5 at the primary side of the transformer

Table 10. Maximum dissipated energy by the LAs for case (2)

Type	Arrester capability [kJ/kV]	Dissipated energy [kJ]					
		Scenario (1)			Scenario (2)		
		Phase					
		A	B	C	A	B	C
3EP5	8	<b>133.13</b>	–	–	4.526	0.083	0.80
3EP6	14	–	–	–	$7.37 \times 10^3$	<b>20</b>	<b>20</b>

is significantly affected by the lightning as shown in Table 10 and Fig. 10 (referring to the affected phase A). The maximum dissipated energy by 3EP5 reaches the value 133.13 kJ, which is sufficient to cause arrester failure since the thermal energy absorption capability of this arrester is 8 kJ/kV. Thus, a higher energy class arrester is required in this case. The sign (–) in Table 10

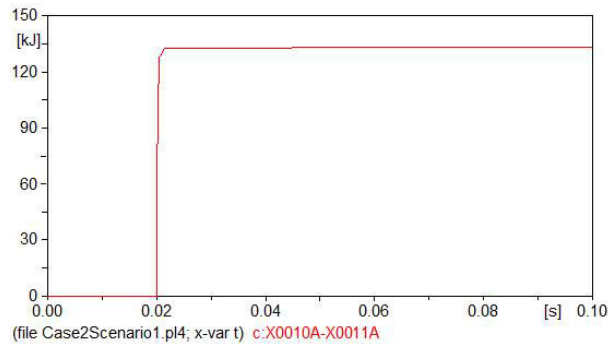


Fig. 10. The energy dissipated by the arrester 3EP5 for phase A (scenario (1) of case (2))

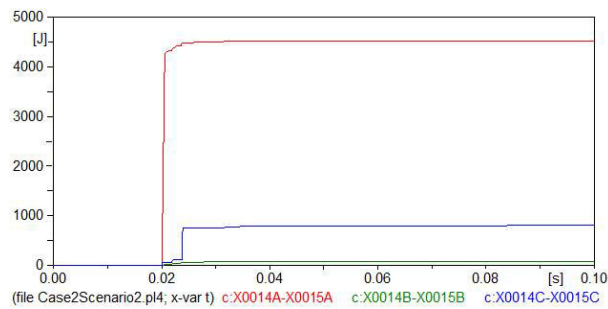


Fig. 11. The energy dissipated by the arrester 3EP5 for the 3 phases (scenario (2) of case (2))

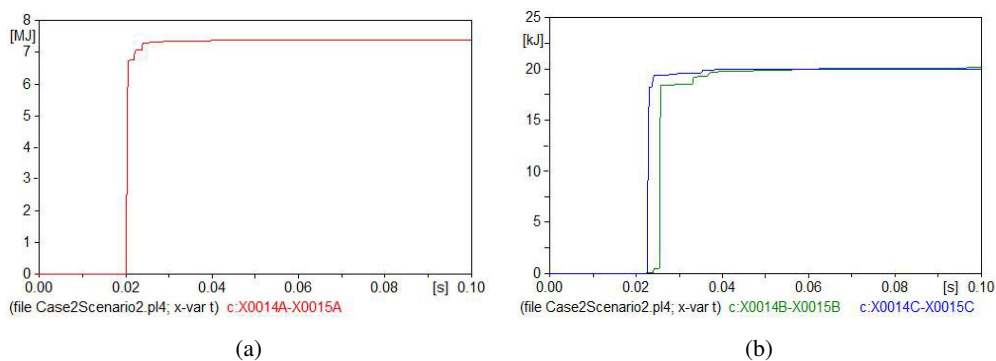


Fig. 12. The energy dissipated by the arrester 3EP6 for phase A (a) as well as phases B and C (b) (scenario (2) of case (2))

indicates neglected value in comparison with the capability of the arrester. For scenario (2), both arresters 3EP5 and 3EP6 are affected by the lightning as shown in Table 10, Fig. 11, and Fig. 12. The maximum dissipated energy by the arrester 3EP5 at the primary side of the transformer is within the thermal energy absorption capability of this arrester. On the other hand, the maximum dissipated energy by the arrester 3EP6 at the secondary side of the transformer reaches the values  $7.37 \times 10^3$  kJ, 20 kJ, and 20 kJ for phases A, B, and C, respectively, which are over the capability of the arrester 3EP6.

## 6. Conclusion

The effect of lightning on the ATPS 15/410 kV power transformers and their protection from lightning is studied using the EMTP-ATP program. The ATPS generators, transformers, underground cables, and the 400 kV transmission line are modeled according to their technical specifications. The results show the destructive impact of lightning on the power transformer without using LAs, where the maximum voltages induced by the lightning flash exceed the transformer BIL, as shown in Fig. 6, Fig. 7 and Table 8.

The study indicates the necessity of installing LAs to both sides of the power transformer. This can be clearly seen in Table 9, where the maximum value of the voltage at the primary side of the transformer is reduced, after the LA installation, from 4.2 MV (for phase A as the worst case – scenario (1) of case (1)) to 97.23 kV, which is within the BIL value (125 kV). Similarly, the maximum value of the voltage at the secondary side of the transformer is reduced from –7.68 MV (for phase A as the worst case – scenario (2) of case (1)) to 1424 kV, which is also within the BIL value (1425 kV).

Finally, according to the results concerning energy absorption issue, as shown in Table 10, a further study can be made to compare different arrester models that are more suitable for the system protection without causing arrester failure due to its thermal energy absorption capability.

## References

- [1] Sroka K., Zlotecka D., *The risk of large blackout failures in power systems*, Archives of Electrical Engineering, vol. 68, no. 2, pp. 411–426 (2019).
- [2] Sclater N., Traister J.E., *Handbook of electrical design details*, Second edition, McGraw-Hill (2003).
- [3] Uman M.A., *The art and science of lightning protection*, Cambridge University Press (2008).
- [4] Choudhuri P., Anderson J.G., Chisholm W.A. et al., *Parameters of lightning strokes: a review*, IEEE Transactions on Power Delivery, vol. 20, issue 1, pp. 346–358 (2005).
- [5] Zoro R., *Tropical lightning current parameters and protection of transmission lines*, International Journal on Electrical Engineering and Informatics, vol. 11, no. 3, pp. 506–514 (2019).
- [6] Heidler F., Flisowski Z., Zischank W. et al., *Parameters of lightning currents given in IEC 62305 – background, experience and outlook*, 29th International Conference on Lightning Protection, Sweden (2008).
- [7] Sestasombut P., Ngaopitakkul A., *Evaluation of a direct lightning strike to the 24 kV distribution lines in Thailand*, Energies, vol. 12, issue 16, p. 3193 (2019).

- [8] Christodoulou C.A., Vita V., Voglitsis D. *et al.*, *Heuristic method for the reduction of the outage rate of high-voltage substations due to atmospheric overvoltages*, Applied Sciences, vol. 8, issue 2, 273 (2018), DOI: 10.3390/app8020273.
- [9] Trainba M., Christodoulou C.A., Vita V., Ekonomou L., *Lightning overvoltage and protection of power substations*, WSEAS Transactions on Power Systems, vol. 12, pp. 107–114 (2017).
- [10] Bak C.L., Einarsdottir K.E., Anderson E. *et al.*, *Overvoltage protection of large power transformers – a real-life study case*, IEEE Transactions on Power Delivery, vol. 23, issue 2, pp. 657–666 (2008).
- [11] Christodoulou C.A., Ekonomou L., Mitropoulou A.D. *et al.*, *Surge arresters' circuit models review and their application to a Hellenic 150 kV transmission line*, Simulation Modelling Practice and Theory, vol. 18, issue 6, pp. 836–849 (2010).
- [12] Prikler L., Hoidalén H.K., *ATPDraw version 5.6, Users' Manual, November 2009*, <http://www.elkraft.ntnu.no/atpdraw/ATPDMan56.pdf>, accessed Dec. 2019.
- [13] Bayadi A., Harid N., Zehar K., Belkhiat S., *Simulation of metal oxide surge arrester dynamic behavior under fast transients*, The International Conference on Power Systems Transients, New Orleans, USA (2003).
- [14] Siemens AG- Energy Sector, *High voltage surge arresters- product guide, 2014*, <https://assets.new.siemens.com/siemens/assets/public.1541967177.cf39125549ad4d35ac7efe44a4173aff75533f1a.catalogue-hv-surge-arresters-en.pdf>, accessed Dec. 2019.
- [15] Bernal J., *Influence of cable lengths on power transformers protection*, Transformers Magazine, vol. 2, issue 3, pp. 82–92 (2015).
- [16] Merz and McLellan consulting engineers, *Technical data for Aqaba power plant/ Generator: WX21Z-092LLT/ Exciter: static*, ABB power generation limited (1996).
- [17] Ali S.A., *Modeling of power networks by ATP-Draw for harmonics propagation study*, Transactions on Electrical and Electronic Materials, vol. 14, no. 6, pp. 283–290 (2013).
- [18] Merz and McLellan consulting engineers, *Aqaba thermal power station – stage II – Main power transformer datasheets*, ABB power generation limited (1996).
- [19] ABB Transformatori S.p.A., *Transformer test report, customer: ABB SAE SADELMI for Aqaba-Jordan* (1996).
- [20] Abdullah M., Ali M.N., Said A., *Towards an accurate modeling of frequency-dependent wind farm components under transient conditions*, WSEAS Transactions on Power Systems, vol. 9, pp. 395–407 (2014).
- [21] Merz and McLellan consulting engineers, *Aqaba thermal power station- stage II – 400 kV cables technical datasheets*, ABB (1996).
- [22] Halasa G., Badran I., El-Zayyat H., *Lightning over-voltages on Amman-Aqaba 400 kV line*, American Journal of Applied Sciences, vol. 4, issue 12, pp. 1075–1078 (2007).
- [23] Uglesic I., *Modeling of transmission line and substation for insulation coordination studies*, Training Dubrovnik, Faculty of Electrical Engineering and Computing, University of Zagreb, Croatia, April (2009).
- [24] IEEE power and energy society, *IEEE standard for general requirements for liquid-immersed distribution, power, and regulating transformers*, 2010, <http://tktransformer.com/wp-content/uploads/2017/07/IEEE-Std-C57.00-2010-IEEE-Standard-for-General-Requirements-for-Liquid-Immersed-Distribution-Power-and-Regulating-Transf.pdf>, accessed Jan. 2020.